Designing Gabor windows using convex optimization

Nathanaël Perraudin *Student Member, IEEE,*, Nicki Holighaus, Peter L. Søndergaard and Peter Balazs *Senior Member, IEEE,*

***Abstract*—Redundant Gabor frames admit an infinite number of dual frames, yet only the canonical dual Gabor system, constructed from the minimal ℓ^2-norm dual window, is widely used. This window function however, might lack desirable properties, such as good time-frequency concentration, small support or smoothness. We employ convex optimization methods to design dual windows satisfying the Wexler-Raz equations and optimizing various constraints. Numerical experiments suggest that alternate dual windows with considerably improved features can be found.**

I. Introduction

Filterbanks, in particular those allowing for perfect reconstruction (PR), are fundamental and essential tools of signal processing. Consequently, the construction of analysis/synthesis filterbank pairs forms a central topic in the literature, relying on various approaches, like polyphase representation [54] or algebraic methods [48]. Other methods rely on frame theory [10], similar to the approach we wish to present. Probably the most widely adopted type of filterbank are modulated cosine and Gabor filterbanks (or transforms) [27], [26], [39], which are closely related. Gabor transforms provide a uniform time-frequency representation by decomposing a signal into translates and modulations of a single *window function*. Such filterbanks have a rich structure, are easy to interpret and allow for efficient computation. A substantial body of work exists on the subjects of invertibility of Gabor filterbanks, perfect reconstruction pairs of Gabor windows and window quality, with a strong emphasis on the overcomplete case [16], [17]. The ability of the analysis filterbank to separate signal components and the precision of the synthesis operation, after coefficient manipulation, depend crucially on the time and frequency concentration of the windows used. While either the analysis or synthesis window can be chosen freely, tuned to the desired properties such as optimal time and frequency concentration, choice of the *dual* window is restricted to the set of functions such that we obtain a PR pair. For computational reasons, detailed below, there is a canonical choice for the dual window, used almost exclusively. However, this *canonical dual window* might not be optimal with regards to the desired criteria, such as time-frequency concentration or short support, required for high quality processing and efficient computation respectively.

Therefore, a flexible method to compute optimal (or optimized) dual windows, considering the full set of possible choices and valid for any set of starting parameters, provides a valuable tool for the signal processing community. We obtain such a method by merging considerations from the theory of Gabor frames with the tools provided by modern convex optimization. The optimization framework we present is not limited to concentration or support optimization, but allows optimization with regards to any criterion that can be expressed through a suitable convex functional. Nonetheless, the aforementioned criteria are of universal importance and well-suited to demonstrate the capabilities and limitations of our method, which is why they form the focus of this contribution.

Since all dual windows perform perfect reconstruction from unmodified Gabor coefficients, the purpose of constructing alternative dual windows might not immediately be obvious beside the minimization of the support. However, if the coefficients are modified, e.g. through signal processing procedures such as frame multipliers [25], [5], [52], also known as Gabor filters [41], the shape of the dual window plays an important role in the quality and localization of the performed modifications. After processing, a signal is synthesized from the modified coefficients employing a dual Gabor filterbank. Let us illustrate the consequences of the window on the synthesis process after modification of the time-frequency representation with a toy example. For this example, we wish to remove an undesirable time-frequency component from a synthetic signal. In Figure 1, we want to remove a localized sinusoid with only minor alteration of the remaining signal. This filtering operation relies on a joint time-frequency representation, since at each time or frequency position, several signal components are active. Although both dual windows, naturally, fail to eliminate the sinusoid completely, they provide visibly different synthesis performance.

In the given example, the first synthesis operation was performed with the canonical dual window, while an alternative dual window with improved time concentration was computed for the second. For redundant Gabor filterbanks, infinitely many alternative dual windows exist, enabling the synthesis system choice based on the requirements of the desired application [7]. Yet, traditional methods utilize the so-called *canonical dual* window, the only dual window that can be obtained directly by applying a linear operator (the inverse

Nathanaël Perraudin (nathanael.perraudin@epfl.ch) is with the Signal Processing Laboratory 2, École polytechnique fédérale de Lausanne, CH-1015 Lausanne, Switzerland

Nicki Holighaus and Peter Balazs are with the Acoustics Research Institute, Austrian Academy of Sciences, Wohllebengasse 12–14, 1040 Vienna, Austria

Peter Søndergaard is with Oticon A/S, 2765 Smørum, Denmark

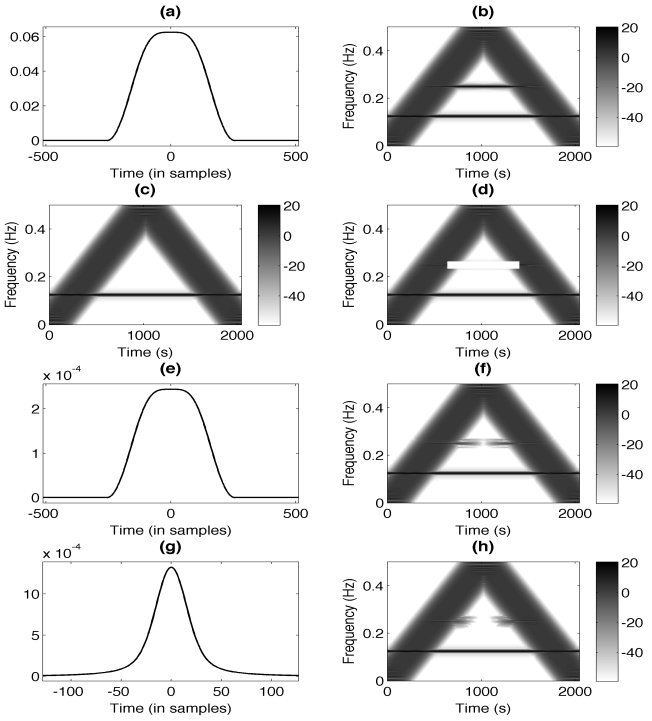

Fig. 1. Reconstruction from modified coefficients: (a) analysis window used to compute the spectrogram[2], (b) Spectrogram of a synthetic test signal, (c) Unachievable 'oracle' target spectrogram, (d) modified spectrogram. (e)(g) 2 different dual windows and (f)(h) spectrograms after synthesis from modified coefficients. Note that the *smearing* effect depends on the concentration of the synthesis window.

frame operator) to the original window.

We propose a convex optimization scheme that selects a dual window such that one or more regularization parameters of the user's choice are optimized. As the solution of a convex optimization problem, the proposed window will be optimal with regards to the selected criteria, provided that the set of admissible dual windows is nonempty.

Innovations of this contribution: We propose a general framework to compute Gabor dual windows satisfying individually selected criteria, expressed in a convex optimization problem. For this purpose, we combine frame-theoretical results with modern convex optimization. In particular, we demonstrate, how our method can be used to provide dual windows with small support, essential for efficient computation, or with optimized time-frequency concentration. Employing various common measures of time-frequency concentration, our experiments show that these criteria can be considerably improved upon the widely-used canonical dual window.

Through the selection of various optimization parameters, our method can be used to explore the set of dual Gabor windows, with the aim to better understand the restrictions imposed by the duality condition.

Finally we introduce a, purely heuristic, method to design tight windows, based on the proposed convex optimization technique. Although the tight window problem is not anymore a convex problem and we lack any convergence guarantee, we observe experimentally that favorable results can be obtained.

The implemented procedure is available as part of comprehensive open-source toolboxes maintained by the authors. An online addendum provides extended computational results and script files reproducing all the presented experiments.

Related work: A wealth of research investigating the subject of dual Gabor windows exists. On the theoretical side, state-of-the-art results are available in [27], [14], support properties of dual windows are investigated in [16], [17], [9], [28] and some specific constructions for dual window pairs are presented in [13], [18], [15], [37], to name a few. Filters optimizing classical window quality measures are constructed in [30], [42], without frame theoretic considerations.

A method for computing dual windows satisfying specific support constraints was proposed by Strohmer [53], based on the Moore-Penrose pseudoinverse of a linear equation system describing duality and the support conditions. The method therein allows the use of other regularization constraints, if these can be expressed through a Hermitian positive definite matrix, e.g. weighted ℓ^2-norms. Already Wexler and Raz [55] impose linear constraints to find alternative dual windows, while Daubechies et al. [23] present a formula for finding dual windows that are optimal in a modified L^2 sense. More similar to our approach, the authors in [38] solve a different convex optimization problem to find sparse dual systems using a weighted ℓ^1-norm. They also provide a method to obtain compactly supported dual windows. This problem is optimized for the research of sparse windows and not suitable for other constraint such as smoothness. With the method proposed in this paper, similar results can be obtained, but sparse dual windows only form a particular example for its possible applications. The existence of sparse dual frames is also investigated in [35], without assuming filterbank structure.

Recently, convex optimization in the context of signal processing has grown into a active field of research and in particular proximal splitting methods [20], [19], [21] have been used to great effect, e.g. in audio inpainting [2], [1] and sparse representation [34]. In those cases, optimization techniques are applied directly to the signal or its time-frequency (TF) representation. In this contribution, we apply optimization techniques to shape the building blocks of the TF representation instead.

Organisation of the paper: This work is an extension of [43]. For the sake of being self-contained, we recall the some results presented therein. We begin by recalling the essential background from convex optimization, as well as important concepts from the theory of Gabor frames. In particular, we recall that the set of dual Gabor windows is characterized by a linear equation system and show that compactly supported dual window pairs are dual independent of the signal length. The convex optimization problem central to our investigation is introduced in Section III, where we also discuss the considered optimization criteria and their effects in the setting of dual Gabor windows. Finally, Section IV

[2]The spectrogram is the squared magnitude of a Gabor-type TF representation.

presents a set of examples designed to illustrate how to use our method for optimizing or adjusting the time and frequency concentration of the dual window for a given starting window. We compare the results visually, in terms of the optimization criteria and classical measures of window quality. Further numerical experiments demonstrate the construction of smmoth dual windows with short support and good frequency concentration and how the proposed optimization scheme can be employed, albeit heuristically, for finding time-frequency concentrated, compactly supported tight windows.

II. Preliminaries

In this contribution, we consider sampled functions, i.e. sequences f in $\ell^2(\mathbb{Z})$ or $\mathbb{C}^L$. The latter is interpreted as the space of L-periodic sequences with indices considered modulo L. For such f, we refer to the smallest closed interval containing all nonzero values of f as its support, denoted by $\mathrm{supp}(f)$. By $x|y$ we denote that $x/y \in \mathbb{Z}$.

Furthermore, we denote *translation* and *modulation* operators

$$\mathbf{T}_n f[l] = f[l-n] \text{ and } \mathbf{M}_\omega f[l] = f[l] e^{2\pi i \omega l},$$

for $f \in \ell^2(\mathbb{Z})$, $l, n \in \mathbb{Z}$ and $\omega \in [0, 1)$. Their counterparts on $\mathbb{C}^L$ are defined in the usual way with indexing modulo L.

A. Convex optimization and proximal splitting

In subsequent sections we design Gabor dual windows as the solution to convex optimization problems of the form

$$\underset{x \in \mathbb{R}^L}{\text{minimize}} \sum_{i=1}^{K} f_i(x), \tag{1}$$

where the f_i belong to a set of convex functions that promote certain features in the solution. Those functions are also referred as *(regularization) priors*. Various methods exist to solve this kind of problem for differentiable priors [29]. However, proximal splitting methods [20] only require the f_i to be lower semi-continuous, convex and proper[3] functions, thus allowing to increase the design's freedom. Those methods solve Eq. (1) by iteratively applying the proximity operator $\mathrm{prox}_f(y) := \underset{x \in \mathbb{R}^L}{\arg\min} \left\{ \frac{1}{2}\|y - x\|_2^2 + f(x) \right\}$ to each prior f_i. More information and convergence results can be found in [47], [40], [20].

Restriction of the optimization to a convex subset $\mathcal{C}$ of $\mathbb{R}^L$, e.g. the set of dual Gabor windows, is achieved by selecting the indicator function

$$i_{\mathcal{C}} : \mathbb{R}^L \to \{0, +\infty\} : x \mapsto \begin{cases} 0, & \text{if } \ x \in \mathcal{C} \\ +\infty & \text{otherwise.} \end{cases}, \tag{2}$$

as prior. Its proximity operator given by the orthogonal projection on $\mathcal{C}$.

[3]A proper function f on a domain C is function satisfying $f(x) > -\infty, \forall x \in C$ and $\exists x \in C$ such that $f(x) < \infty$

B. Gabor systems, frames and dual windows

We define the Gabor system

$$\mathcal{G}(g, a, M) := \left(g_{m,n} = M_{m/M} T_{na} g\right)_{n \in \mathbb{Z},\ m=0,\ldots,M-1} \tag{3}$$

for a given window $g \in \ell^2(\mathbb{Z})$, a hop size $a \in \mathbb{Z}$ and a number of frequency bins $M \in \mathbb{Z}$.

For any signal $f \in \ell^2(\mathbb{Z})$, the *Gabor coefficients* (or Gabor analysis) with respect to $\mathcal{G}(g, a, M)$ are given by

$$(\mathbf{G}f)[m + nM] = \langle f, g_{m,n} \rangle = \sum_{l \in \mathbb{Z}} f[l] \, \overline{g_{m,n}[l]}, \tag{4}$$

with the analysis operator $\mathbf{G}$ given by the infinite matrix $\mathbf{G}[m + nM, l] := \mathbf{G}_{g,a,M}[m + nM, l] := \overline{g_{m,n}[l]}$.

Gabor synthesis of a coefficient sequence $c \in \ell^2(\mathbb{Z})$ with respect to $\mathcal{G}(g, a, M)$ is performed by

$$f_{syn}[l] = (\mathbf{G}^* c)[l] = \sum_{n \in \mathbb{Z}} \sum_{m=0}^{M-1} c[m + nM] \, g_{m,n}[l], \tag{5}$$

where $\mathbf{G}^*$ denotes the transpose conjugate of $\mathbf{G}$. In $\mathbb{C}^L$, a Gabor transform with $a = 1$ and $M = L$ is also known as (full) *short-time Fourier transform* (STFT). This highly overcomplete setup allows for straightforward inversion using the synthesis operator, i.e. $f = \mathbf{G}^* \mathbf{G} f$, however [27]. Otherwise, we require that $\mathcal{G}(g, a, M)$ forms a stable, (over-)complete system satisfying

$$A\|f\|_2^2 \leqslant \|\mathbf{G}f\|_2^2 \leqslant B\|f\|_2^2, \text{ for all } f \in \ell^2(\mathbb{Z}), \tag{6}$$

for some $0 < A \leqslant B < \infty$, i.e. a *Gabor frame* [14]. In that case, every signal $f \in \ell^2(\mathbb{Z})$ can be written as

$$f = \mathbf{G}^*_{g,a,M} c \tag{7}$$

for some coefficient sequence $c \in \ell^2(\mathbb{Z})$. A frame is *tight*, if $A = B$ is a valid choice. The frame property guarantees the existence of a dual Gabor frame $\mathcal{G}(h, a, M)$ such that $f = \mathbf{G}^*_{h,a,M} (\mathbf{G}_{g,a,M} f) = \mathbf{G}^*_{g,a,M} (\mathbf{G}_{h,a,M} f)$ holds for all $f \in \ell^2(\mathbb{Z})$. Hence, c in (7) can be chosen to be the Gabor coefficients with respect to $\mathcal{G}(h, a, M)$.

If $\mathcal{G}(g, a, M)$ is redundant, then the *dual window* $h \in \ell^2(\mathbb{Z})$ is not unique. Instead, the space of dual windows equals the solution set of the *Wexler-Raz (WR) equations* [55], [50], that characterize the dual Gabor windows for $\mathcal{G}(g, a, M)$. They are given by

$$\begin{aligned} \frac{M}{a} \left\langle h, g[\cdot - nM] e^{2\pi i m \cdot / a} \right\rangle = \delta[n]\delta[m] \\ \text{or } \mathbf{G}_{g,M,a} h = [a/M, 0, 0, \ldots]^T, \end{aligned} \tag{8}$$

for $m = 0, ..., a-1, \ n \in \mathbb{Z}$. Here, δ denotes the Kronecker delta. Note that, while $\mathbf{G}_{g,a,M}$ is overcomplete, $\mathbf{G}_{g,M,a}$ is underdetermined and admits infinitely many solutions, whenever $a < M$.

The WR equations form the central step towards the formulation of the Gabor dual problem in the context of convex optimization. Any function in this set facilitates perfect reconstruction from unmodified coefficients, but some are better suited for synthesis from processed coefficients than others, see Figure 1. From now on, we will denote by $\mathcal{C}_{dual}$ the

solution set of the nontrivial WR equations, forming the basic constraint of the considered optimization problem.

The *canonical dual window*, defined via the pseudo-inverse of the analysis operator $\mathbf{G}_{g,a,M}$, is the only widely used dual. It can be computed efficiently, see e.g. [8], [31]. We note that the canonical dual window γ minimizes the ℓ^2-norm as well as the ℓ^2-distance to g among all duals, see e.g [27, Prop. 7.6.2]. Unless certain very specific conditions are satisfied, the canonical dual is infinitely long [9], preventing finite time synthesis. The most prominent setup that provides a compactly supported canonical dual is the *painless case*, i.e. when the length of g is less or equal than the number of channels M. Therefore the setup where the length of the window equals the number of channels is omnipresent in signal processing, to the point where these two numbers are sometimes not distinguished. For integer redundancy, the conditions in [9] are even equivalent to the painless case.

Gabor dual windows beyond the canonical dual: A considerable amount of research on alternative Gabor dual windows has been conducted, mostly concerned with finding dual pairs of windows with compact support. Such results often consider special configurations of analysis window [18], [37] and/or Gabor parameters [13], [16], [17]. While compactly supported duals play a central role in this contribution, our method admits further design's freedoms and does not impose constraints on the analysis window or on Gabor parameters. To ensure efficient computation, it is crucial to establish the independence of the duality conditions for compactly supported pairs of dual windows from the signal length L. This property, while widely accepted in the community, seems not to have found its way into the literature explicitly. Since it forms a central point of our argument, we will now state the result including a short proof. We now assume the existence of finite intervals I_g, I_h such that $\operatorname{supp}(g) \subseteq I_g$ for the analysis window and $\operatorname{supp}(h) \subseteq I_h$ for the solution dual window.

Lemma 1. *Let I_g, I_h be intervals of length L_g and L_h with nonempty intersection. For any Gabor system $\mathcal{G}(g,a,M)$ with $\operatorname{supp}(g) \subseteq I_g$ and any $h \in \ell^2(\mathbb{Z})$ with $\operatorname{supp}(h) \subseteq I_h$, all but $a\lceil \frac{L_g+L_h}{M} \rceil$ of the WR equations are trivally satisfied. Moreover, if $\langle h, g\rangle_{\ell^2} = a/M$, then the following are equivalent:*

(i) *g, h are Gabor dual windows on $\ell^2(\mathbb{Z})$ for a, M,*
(ii) *For any $L > L_g + L_h$ with $a, M \mid L$, g_{fin}, h_{fin}, defined by $g_{fin}[l] = \sum_{k\in\mathbb{Z}} g[l-kL]$ and $h_{fin} = \sum_{k\in\mathbb{Z}} g[l-kL]$ for $l = 0, \dots, L-1$, are Gabor dual windows on $\mathbb{C}^L$ for a, M.*

Moreover, (i)⇒(ii) holds for any $L \geqslant L_g, L_h$ with $a, M \mid L$.

Proof: By assumption there are $n_0, n_1 \in \mathbb{Z}$, with $n_0 \leqslant 0 \leqslant n_1$ such that $I_g \cap (I_h + nM) \neq \varnothing$ for $n_0 \leqslant n \leqslant n_1$ and $I_g \cap (I_h + nM) = \varnothing$ for every other $n \in \mathbb{Z}$. In particular, $n_1 - n_0 \leqslant \lceil \frac{L_g+L_h}{M} \rceil - 1$. Therefore $\langle h, \mathbf{M}_{ma^{-1}} \mathbf{T}_{nM} g\rangle = 0$ for all $n \in \mathbb{Z}$ s.t. $n < n_0$ or $n > n_1$, proving that at most $a\lceil \frac{L_g+L_h}{M} \rceil$ of the WR equations are not trival. Now let $L \in \mathbb{N}$ such that $L > L_g + L_h$ and $M \mid L$. It is easily seen that

$$\langle h_{fin}, \exp(2\pi i m \cdot /a) \mathbf{T}_{nM} g_{fin}\rangle_{\mathbb{C}^L} = \langle h, \mathbf{M}_{ma^{-1}} \mathbf{T}_{nM} g\rangle_{\ell^2} \tag{9}$$

holds for all $m = 0, \dots, a-1$ and $n_0 \leqslant n \leqslant n_1$, proving (ii)⇒(i). Note that translation on the left side of the equation is circular and $L > L_g + L_h$ guarantees that the sums defining $g_{fin},\ h_{fin}$ possess only a single nonzero term each. To prove (i)⇒(ii), observe that $L > L_g + L_h$ implies $\langle h_{fin}, \exp(2\pi i m \cdot /a) \mathbf{T}_{nM} g_{fin}\rangle_{\mathbb{C}^L} = 0$ for $n_1 < n < L/M - n_0$. For the final part, assume for now that $I_g,\ I_h$ are centered around 0. If $L \geqslant L_g, L_h$ and $a, M \mid L$, then the sums defining $g_{fin},\ h_{fin}$ possess only a single nonzero term each still and

$$\begin{aligned}\delta[n]\delta[m] &= \left\langle h_{fin}, g_{fin}[\cdot - nM] e^{2\pi i m \cdot /a} \right\rangle \\ &= \begin{cases} \left\langle h, \mathbf{M}_{m/a} \left(\mathbf{T}_{nM}\, g + \mathbf{T}_{(nM+L)}\, g \right) \right\rangle & \text{if } nM \leqslant L/2, \\ \left\langle h, \mathbf{M}_{m/a} \left(\mathbf{T}_{nM}\, g + \mathbf{T}_{(nM-L)}\, g \right) \right\rangle & \text{if } nM > L/2. \end{cases}\end{aligned}$$

If either, or both, of $I_g,\ I_h$ are not containing 0, the result is obtained by a suitable index shift in n. ∎

Compactly supported duals by truncation: In 1998, Strohmer proposed a simple algorithm for the computation of compactly supported dual windows when a compactly supported analysis window is given [53]. The algorithm, which we will refer as the *truncation method*, requires no additional restrictions to the analysis system, similar to our own approach. The truncation method is based on the fact that a support constraint on the dual window is equivalent to deleting the corresponding columns in the WR matrix (8) and computing only the values that are possibly nonzero. The resulting equation system is then solved by computing the pseudoinverse, obtaining the least-squares solution. While the resulting windows satisfy the duality conditions, they are not very smooth and indeed show some discontinuity-like behaviour, see Figure 11(e,f). One of the goals of this contribution is the improvement of these undesirable effects.

Strohmer's method is not restricted to support constraints, but can be adjusted for the direct computation of a dual window $h \in \mathcal{C}_{dual}$ that minimizes $\|\mathbf{R}h\|_2$, for some Hermitian positive definite matrix $\mathbf{R}$. However, [53] does not explore this possibility beyond the proposition of weighted ℓ^2-norm optimization and the method remains more restrictive than a general convex optimization formulation.

III. Design of optimal dual windows

For a given Gabor frame $\mathcal{G}(g,a,M)$ the construction of a suitable Gabor dual window supported on an interval I_h can be accomplished by solving

$$\operatorname*{arg\,min}_{x \in \mathcal{C}_{\text{dual}} \cap \mathcal{C}_{\text{supp}}} \sum_{i=1}^{K} f_i(x), \tag{10}$$

where $\mathcal{C}_{dual}$ is the set of dual windows, $\mathcal{C}_{supp}$ the set of all functions in $\ell_2(\mathbb{Z})$ supported on I_h and f_i are priors that promote certain features in the solution. In practice, each f_i is weighted by a regularization parameter $\lambda_i > 0$ for tuning the quantitative relations between the priors. Moreover, we only consider real-valued, symmetric windows g and real-valued solutions. Those two supplementary constraints are not mandatory for optimization. However, they are used in most applications. For real-valued g, the canonical dual window is guaranteed to be real-valued, as a direct consequence of

the Walnut representation of the Gabor frame operator [14]. Hence, the set of real-valued dual windows is a non-empty affine subspace of all dual windows. Note that the constraint $x \in \mathcal{C}_{supp}$ can be dropped if a solution only for a specific finite dimensional setup is required. However, when a dual window for $\ell_2(\mathbb{Z})$ or independent from the signal length L is desired, the finite support constraint is mandatory. Beyond this consideration however, reduced support $L_h \ll L$ is often desired to improve the efficiency and to shorten the processing delay. Another minor decrease in complexity can be obtained by reducing the number of frequency channels M, while keeping the redundancy M/a fixed, thus favoring non-painless configurations.

The process of selecting and tuning the priors f_i is very flexible and therefore heavily dependent on the intended application, which is reminiscent of the situation for the search of the *optimal* window. Here, we will mainly investigate the optimization of several classical measures of time, frequency and TF concentration. This problem is of particular importance, since joint TF concentration (or equivalently TF smoothness) is crucial for the minimization of artifacts, when performing local modification of TF coefficients in processing application. A list of the priors we consider is provided in Table I and their effect is discussed in the next section.

Remark 1. *For a solution to* (10) *to exist, obviously* $\mathcal{C}_{dual} \cap \mathcal{C}_{supp} \neq \varnothing$ *is required. It is known [53] that the WR equations are linearly independent. The same can easily be seen for the equations describing the support set* $\mathcal{C}_{supp}$*. However, when jointly considering both equation systems, we have observed linear dependencies for nonrandom analysis windows. Linear dependencies can theoretically lead to unsolvable systems or additonal degrees of freedom. However, in practice, we have only observed the latter and controlling the number of equations is usually sufficient for ensuring solvability, but might not be optimal in the sense of minimality. An investigation of this issue is planned for a later contribution.*

A. Functionals and proximal operators

In order to tune the solution of a convex optimization problem (10) towards the properties we desire, we have to select *priors* f_i that promote these properties. In this contribution, we mostly consider priors that are fairly standard in optimization, or simple extensions of such priors. Although their various effects are quite well known, e.g. ℓ^1 optimization favors solutions with a few large values while an ℓ^2 prior favors a more even spread of the energy, considerable limitations are imposed by the duality constraint. Although the set of Gabor dual windows is characterized by the WR equations, their implications in terms of window shape, localization, decay etc. remain largely unexplored. Therefore a short discussion of relevant priors, expected effects and their actual effect in our context seems worthwhile.

All the examples provided in this section were computed with an Itersine[4] analysis window with $L_g = 60$ $L = 240$, $a = 15$ and $M = 120$, without support constraints. This setup, in particular its high redundancy, allows us to shape the dual windows rather freely for different objective functions, therefore producing characteristic examples. The window is shown in Fig. 2. The canonical dual (not depicted), equals the window up to scaling.

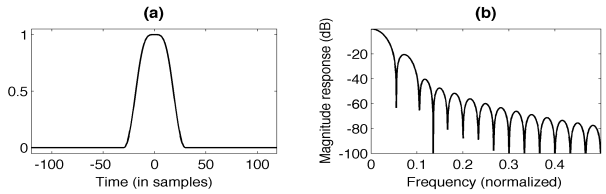

Fig. 2. The Itersine window and its magnitude frequency response (in dB).

ℓ^1-norm minimization is usually considered, whenever (approximate) sparsity, i.e. a small number of (significant) non-zero values is desired. As the convex relaxation of the ℓ^0 minimization problem, it is equivalent or at least close to sparsity optimization under certain conditions [38], [12]. In general, these conditions are not satisfied by Eq. (10). Nevertheless, the restrictions imposed by the WR equations usually allow a solution with few large values. It should be noted however, that small ℓ^1-norm does not imply clustering of the large values, i.e. a solution supported on a short interval. As expected, some concentration is induced by the duality constraint, see Fig. 3 (a)(b). In the presented experiment, the ℓ^1 solution possesses only 15 values above -80 dB (relative to the maximum amplitude) on an interval around 0, only half the number of WR equations $\frac{L}{M}a = 30$. However, other configurations have provided solutions with few significant values spread over a larger interval, see the webpage.

The proximity operator of the ℓ^1 prior is computed by soft-thresholding:

$$\mathrm{soft}_\mu(y) = \mathrm{sgn}(y)\,(|y| - \mu)_+$$

where $(\cdot)_+ = \max(\cdot, 0)$. For compactly supported windows, a strictly bandlimited dual window is usually not feasible. Therefore, when applied in the Fourier domain, the ℓ^1 prior cannot achieve a truly sparse solution, but promotes a small number of significant values. In many cases, the result is similar to actual concentration measures, compare Fig. 3(c)(d) and Fig. 5(a)(b).

An ℓ^2 prior will, in our context, always lead to the canonical dual Gabor window. In general, this prior will affect the values in a more proportional way over the whole signal range. It is traditionally used as a data fidelity term, i.e. the solution is expected to be close, in the ℓ^2-norm sense, to a given estimate. The associated objective function is not only convex, but also smooth, admitting gradient descent approaches for minimization.

[4]The Itersine window $g(t) = \sin(0.5\pi \cos(\pi t)^2)\chi_{[-1/2,1/2]}$, where χ_I is the characteristic function of I, is designed to form a tight frame in the painless case with half overlap. This is equivalent to the sum of the squared modulus of the translated windows summing to a constant, a property that is retained for any appropriately sampled version.

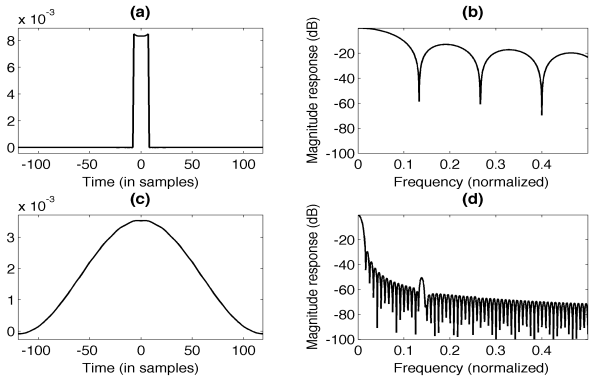

Fig. 3. Result of ℓ_1 optimization. Priors: (a)(b) $\|x\|_1$ (c)(d) $\|\mathcal{F}x\|_1$

a) Concentration inducing functions: Our main objective in the following section will be the search for a Gabor dual window with optimized/modified TF concentration. Therefore we recall a number of different concentration measures Inspired by the famous Heisenberg inequality, the most natural way to impose localization is to optimize the variance of the signal $x \in \mathbb{R}^L$ or more precisely, its modulus:

$$\text{var}(|x|) = 1/\sqrt{L} \sum_{i=-L/2}^{L/2-1} (i - \overline{|x|})^2 |x_i|$$

with $\overline{|x|} = \sum_{i=-L/2}^{L/2-1} i|x_i|$ being the center of gravity. As we consider symmetric windows $\overline{x} = 0$, we can simplify this expression to: $\text{var}(|x|) = 1/\sqrt{L} \sum_{i=-L/2}^{L/2-1} (i)^2 |x_i|$. In that case[5], the variance turns out to be a weighted ℓ^1-norm with quadratic weight w^2, $w := \frac{1}{\sqrt{L}} [-L/2, \ldots, L/2-1]$. Compared to ℓ^1 minimization, this prior additionally penalizes values far from the origin, inducing concentration. The proximity operator of $\text{var}(|x|)$ is a variation of the ℓ^1 proximity operator and computed by weighted soft thresholding. And example is shown in Fig. 4(a)(b).

We also consider the variance of the energy of the signal: $\text{var}(|x|^2)$, for symmetric windows equal to a weighted ℓ^2 norm with linear weight w: $\text{var}(x^2) = \|w \cdot x\|_2^2$. Explicit computation of the proximity operator leads to

$$\text{prox}_{\gamma \text{var}(x^2)}(y) = \frac{1}{1 + 2\gamma w^2} y, \tag{11}$$

i.e. multiplication with a function that decays quadratically away from zero, see Fig. 4(c)(d).

A closely related concentration measure is smoothness in frequency, as measured by the gradient of the Fourier transform $\|\nabla \mathcal{F}x\|_2^2$. Indeed, the resulting proximity operator has almost the same form:

$$\text{prox}_{\gamma \|\nabla \mathcal{F}x\|_2^2}(y) = \frac{1}{1 + 2\gamma \psi} y \tag{12}$$

with $\psi[l] = 2 - 2\cos\left(\frac{2\pi l}{L}\right)$. Since $\psi[l] \approx Cl^2$ for small l and values away from 0 are strongly attenuated, the priors $\text{var}(|x|^2)$ and $\|\nabla \mathcal{F}x\|_2^2$ often lead to similar results. Both functions induce concentration by attenuation of values far from the origin. Examples are shown in Fig. 4(e)(f).

Concentration in frequency is easily achieved through $\text{var}(|\mathcal{F}x|)$, $\text{var}(|\mathcal{F}x|^2)$ or $\|\nabla x\|_2^2$. The respective proximity operators are obtained simply by conjugating the proximitiy operators discussed above with the (inverse) Fourier transform. For examples, see Fig. 5.

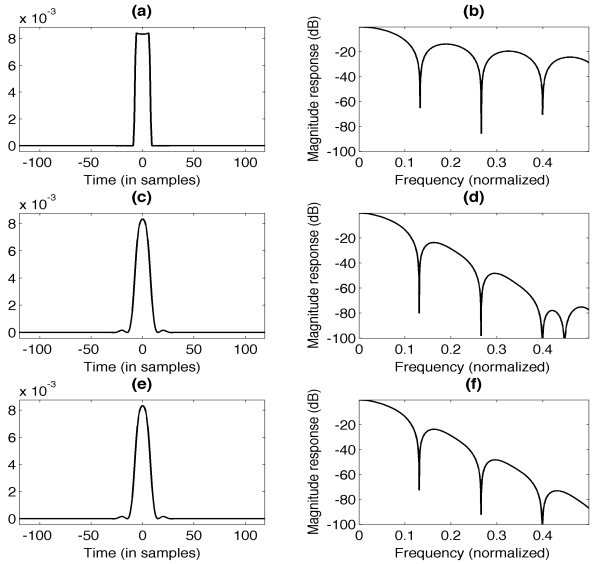

Fig. 4. 'Time-optimized' dual windows and their magnitude frequency response (in dB). Priors: (a)(b) $\text{var}(|x|)$. (c)(d) $\text{var}(|x|^2)$. (e)(f) $\|\nabla \mathcal{F}x\|_2^2$

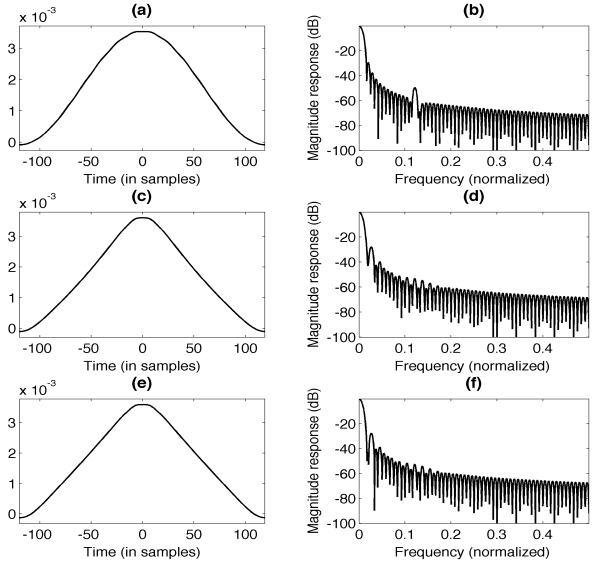

Fig. 5. 'Frequency-optimized' dual windows and their magnitude frequency response (in dB). Priors: (a)(b) $\text{var}(|\mathcal{F}x|)$. (c)(d) $\text{var}(|\mathcal{F}x|^2)$. (e)(f) $\|\nabla x\|_2^2$

b) Concentration in time and frequency: For simultaneous concentration in time and frequency, we can consider jointly the time- and frequency-domain variants of the priors discussed above. Alternatively, we use a single cost functions providing concentration in both domains at once. In TF literature, modulation space norms, i.e. ℓ^p norms on the short-time Fourier coefficients are frequently used to measure joint TF localization, see e.g. [27], [24]. In particular $\|x\|_{S_0} =$

[5]If the center of gravity is not fixed to 0, the variance is not a weighted ℓ_1 norm anymore and its optimization is not straightforward. For a symmetric prototype, it is reasonable to assume the center of gravity of the dual window to coincide with the $\overline{|g|}$.

$\|G_{g,1,L}x\|_1$, where g is a Gaussian function, is considered as quality measure for window functions. Minimization of the S_0-norm can be expected to yield TF concentrated windows. However, similar to the ℓ^1-norm, small S_0-norm does not guarantee concentration around the origin (or any single TF location). As expected, the duality constraint seems to enforce some localization, though.

Compared to the previously discussed priors, S_0 optimization is considerably more expensive. Since we are not aware of a explicit solution to the S_0 proximity operator, we propose its computation via an iteration based on ADMM [11]. The number of required ADMM steps per PPXA iteration is low and scales well with L (usually 3-4 steps provided sufficient precision), but each substep requires the computation of one full STFT and one inverse STFT, with a complexity of $\mathcal{O}(L^2 \log(L))$ each. An example for S_0 optimization is shown in Fig. 6(a)(b).

In some cases, concentration can be further increased by S_0-norm instead. The proximity operator is realized similar to the unweighted case. Fig. 6(c)(d) shows an example using the circular weight

$$W[f,t] = \ln\left(1 + w^2[t] + w^2[f]\right),$$

using the weight w as defined above. While other weights are clearly feasible, the weight above has been tuned to yield good results in our experiments and is also used for Exp. 1.

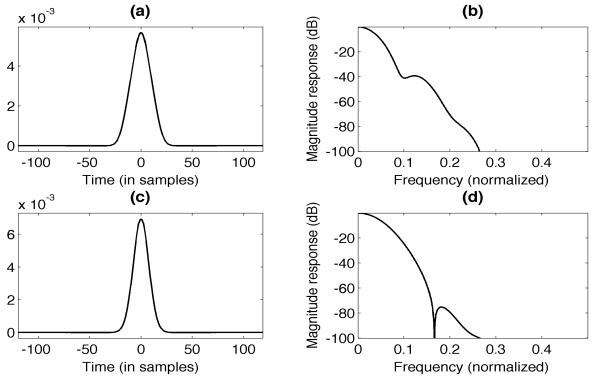

Fig. 6. Result of optimization function $\|x\|_{S_0} = \|G_{g,1,L}x\|_1$ (a)(b) and its weighted version (c)(d)

c) Other cost functions: The list of possible cost functions is vast and the full exploration of the possibilities of convex optimization in window design is far beyond the scope of any single contribution. As a rather academic example, we propose a free design approach that selects the dual Gabor window closest to the linear span of a model window g_{sh}, i.e. we find

$$\underset{x \in \mathcal{C}_{\text{dual}}}{\arg\min} \|x - P_{\langle g_{sh} \rangle} x\|_2^2,$$

where $\langle g_{sh} \rangle$ is the linear span of $g_s h$. The solution is computed by a POCS (projection onto convex set) [22] algorithm. Due to the examples academic nature, we were not concerned with convergence time. Examples using a sine wave and a dirac pulse as model window are presented in Fig. 7(a)(b) and (c)(d)(d').

A note on implementation and complexity: Various methods exist for solving the optimization problems formulated throughout the paper, e.g. generalized forward backward [45] or SDMM [49] [20], some of which might prove more efficient than the parallel proximal algorithm (PPXA) [19] which we employ. However, optimizing computational complexity is, for several reasons, not at the center of this contribution. First, in contrast to continuously varying the analysis window and transform parameters, a single (or few different), predetermined transform configuration is usually used repeatedly, allowing for off-line computation of the dual window in

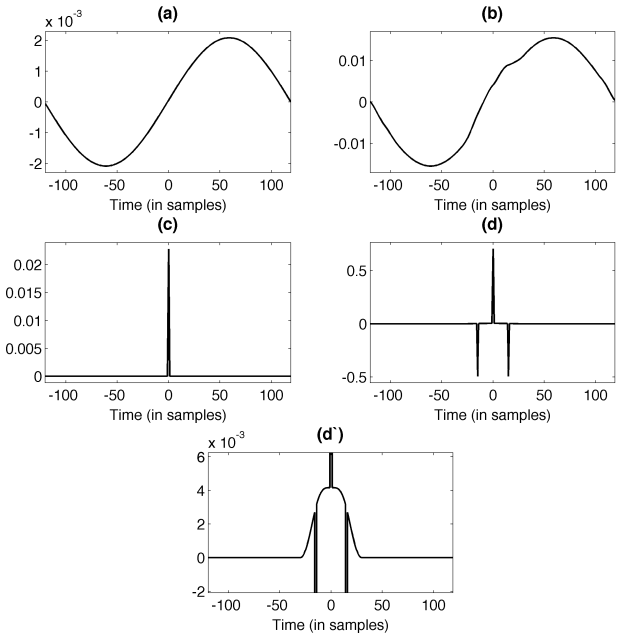

Fig. 7. Result of optimization function $\|x - P_{\langle g_{sh} \rangle} x\|_2^2$. g_{sh} (left) and the result of optimization (right): : (a)(b) A sine. (c)(d) An impulse (Dirac). Note that the solution window (d) is actually composed of a smooth bump function in addition to the 3 clearly visible impulses. We provide a zoom-in in (d'). .

TABLE I
SUMMARY OF IMPORTANT PRIORS

Function	Effect on the signal	Complexity
$\|x\|_1$	sparse representation in time	L
$\|\mathcal{F}x\|_1$	sparse representation in frequency	$L\log(L)$
$\|\nabla x\|_2^2$	smoothen in time / concentrate in frequency	$L\log(L)$
$\|\nabla \mathcal{F}x\|_2^2$	smoothen in frequency / concentrate in time	L
$\|x\|_{S0}$	Concentrate in both time and frequency	$L^2\log(L)$
$\|x\|_2^2$	spread values more evenly/ toward the canonical dual	L
var$(\|x\|)$	Concentrate the signal in time	L
var(x^2)	Concentrate the signal in time	L
var $(\mathcal{F}x)$	Concentrate the signal in frequency	$L\log(L)$
var $\left((\mathcal{F}x)^2\right)$	Concentrate the signal in frequency	$L\log(L)$
$i_{\mathcal{C}}(x)$	force $x \in \mathcal{C}$	L^2 $[L^3]$

advance. Second, our main concern is the construction of pairs of dual windows such that duality is satisfied independent of the signal length L_s by imposing support constraints, see Section II-B. Therefore, the complexity depends mainly on the support size of the dual windows and not of the signal size L_s. This is theoretically shown in Lemma 1. Third, most of the applications use windows of size smaller than 10^4 samples, where the implementation used provides quick converge, except for the S_0-norm prior, which might require several minutes of computation time.

The complexity of the overall algorithm depends mostly on the computation of the proximal operator of the selected priors. Indeed, the most expensive prior operator is often the bottleneck of the optimization algorithm (whereas the choice of the algorithm itself influences more the total number of iterations). For very large L, the algorithm will be limited by the projection onto the dual set satisfying the WR systems of equations $Gx = \delta$. The solution of the projection

$$\arg\min_x \|x - x_0\|_2^2 \quad \text{s. t. } Gx = \delta,$$

is given by

$$x = x_0 - G^* \left(GG^*\right)^+ \left(Gx_0 - \delta\right).$$

The projection itself has quadratic complexity, but the pseudoinverse of the matrix GG^* has to be computed before the start of the iteration process. This particular computation scales with L^3. Due the the rarity of requiring very long windows, this is usually no limitation. The complexity of the other proximal operators is provided in Table I. Among the those, we do observe that the optimization of the (weighted) S_0 norm is much more expensive. As a results, it might be preferable to optimize both the separable time-frequency measures instead, leading to a complexity of $O(L\log(L))$ instead of $O(L^2\log(L))$.

IV. Numerical experiments

In the following sections, we present several experiments providing dual Gabor windows optimizing joint TF concentration. Such windows are well-suited both as analysis and synthesis windows, reducing cross-component interference in the Gabor coefficients or increasing the precision of processing operations, respectively. It is widely known that windows of Gaussian type $g(t) = e^{-ct^2}$ optimize a wide variety of concentration measures, such as the Heisenberg uncertainty (product of variances), $\|g\|_{S_0}/\|g\|_2$ and many more [46]. The same can be said about its discretized couterpart. However, Gaussian windows are not compactly supported in either domain and any attempt to make them so has a detrimental effect on the TF concentration. Compact support in either domain generally introduces infinite support and oscillation in the other, but low amplitude values (in comparison to the desired processing precision) can often be considered irrelevant. Therefore the concept of a *good* window depends not only on the application, but on the user as well.

We now present 3 experiments where we compute various *optimal* dual windows under different assumptions and restrictions. Exp. 1 provides a comparison of the effect of the concentration measures discussed in Sec. III-A, when applied jointly in time and frequency. Exp. 2 demonstrates, by tuning the optimization parameters, that the set of dual windows allows surprising freedom when choosing the trade-off between time and frequency concentration. In those two first experiments we impose only a weak support constraint (i.e the support of the dual is longer than the support of the analysis window). In contrast to the previous experiments, Exp. 3 considers a situation beyond the painless case, i.e. the canonical dual window has long (possibly infinite) support. We construct a smooth dual window h supported I_g, the support set of g and compare our result to that provided by the truncation method.

Simulations were performed using the LTFAT [51] and the UNLocBoX Matlab toolbox [44]. A reproducible research addendum with additional material and MATLAB scripts that reproduce the presented results is available in http://unlocbox.sourceforge.net/rr/gdwuco. We refer to this address as the *webpage*.

Experiment 1 - Optimizing TF concentration: In this experiment, we simultaneously optimize TF concentration with regards to the previously introduced measures. This is either achieved by a single prior on the TF representation of the dual window h ($\|x\|_{S_0}$, $\|x\|_{S_0,w}$, or by applying the time and frequency versions of one prior, with equal weights ($\|\nabla x\|_2^2$, var($|x|$), var($|x|^2$)), i.e.

$$\arg\min_{x\in\mathcal{C}_{\text{dual}}\cap\mathcal{C}_{\text{supp}}} f(x) + f(\mathcal{F}x).$$

The time step γ of the algorithm has been tuned experimentally for each prior, to yield good convergence speed and precision. For this experiment, we have chosen a Tukey window with a transition area ratio[6] of $3/5$ (see Fig. 8, with $L_g = 240$, $a = 50$ and $M = 300$. The support of the dual window candidates was restricted to $L_h = 600$.

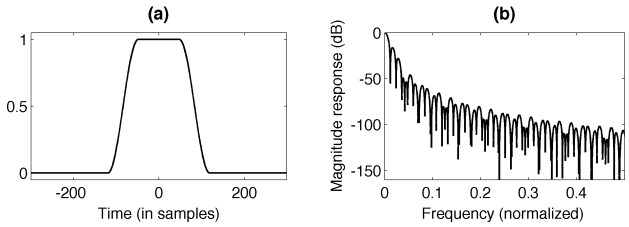

Fig. 8. The analysis Tukey window and its magnitude frequency response (in dB).

Fig. 9 shows time and frequency representations, as well as the ambiguity function[7] of the results. We see that all the criteria provide (visually) nicely concentrated dual Gabor windows, improved over the canonical dual, Fig. 9(a)(b)(c). In particular, we see that the gradient and energy variance optimal windows are very similar around the origin, whereas

[6]The Tukey window with transition area ratio $r \in [0,1]$ is given by $g(t) = 1$ for $t \in [-(1-r)/2, (1-r)/2]$, $g(t) = 0.5 + 0.5\cos(\pi(2t - r + 1)/2r)$ for $t \in [-1/2, -(1-r)/2]$, $g(t) = 0.5 + 0.5\cos(\pi(2t + r - 1)/2r)$ for $t \in [(1-r)/2, 1/2]$ and zero else.

[7]In $\mathbb{C}^L$, the ambiguity function is the STFT of a function with regards to itself: $\mathcal{G}(f, 1, L)f$.

the latter shows worse decay. The variance induces the best concentration of large values in an almost rectangular TF area, but similar to the energy variance, no good decay is achieved. Both S_0 and weighted S_0 priors perform very well, but the weight induces a more symmetric TF concentration and slightly better decay.

Note that, while the shape of this experiment's results is quite characteristic, their quality cannot be representative for any arbitrary setup. In fact the results are highly dependent on the quality of the original Gabor frame, its redundancy and the choice of support constraint. As expected, the optimization effect is smaller, the better your starting point is. For additional experiments with other starting windows and/or without support constraint, we refer to the webpage.

To further emphasize the similarities and differences between the window functions and to assess their quality, we computed for all the results every concentration measure discussed in Sec. III-A, see Table II. Besides demonstrating nicely that the various solutions actually provide the best result in their respective criteria, the table underlines the similarity of gradient and energy variance optimization. In total, except for the canonical dual and S_0-norm solution, all results are reasonably close. The different shape of the S_0-norm solution is easily explained is easily explained by the fact that it is the only measure that does not penalize high energy away from the origin. Furthermore, in Table III, the following classical measures for window quality are presented: -3 dB width (time), main lobe width (frequency), side lobe attenuation (frequency, in dB) and side lobe decay (in dB). Please note that the lack of an underlying continuous function for the dual windows prevents us from determining the side lobe decay rate from the degree of smoothness of the window. Therefore, as a rough approximation, we compute the ratio between the largest sidelobe and the largest of the final 3 side lobes below the Nyquist frequency instead. Notably, the variance optimization concentrates that main energy contribution in the smallest TF area as indicated in th third column, while the gradient optimization provides arguably the most balanced solution and the best decay properties, followed by the considerably more expensive S_0 and weighted S_0 solutions.

Experiment 2 - Controlling the time-frequency trade-off: It is well known that no function can be arbitrarily concentrated in both the time and the frequency domain simultaneously. When choosing a dual window to a given Gabor frame the concentration is further limited by the duality conditions, the shape and the quality of the given frame. Oversimplified, a badly conditioned Gabor frame (with large frame bound ratio B/A), admits only badly concentrated duals. However, even if the canonical dual window is well concentrated overall, applications might benefit from the improvement of time concentration versus frequency concentration and vice-versa. To see this, just recall that the TF shape of the synthesis window limits the precision of TF processing.

The following experiment demonstrates the surprising flexibility that the set of dual windows allows when choosing the appropriate TF concentration trade-off. The system parameters are the same as in Exp. 1: $L_g = 240$, $a = 50$, $M = 300$ and dual window support less or equal to $L_h = 600$. However,

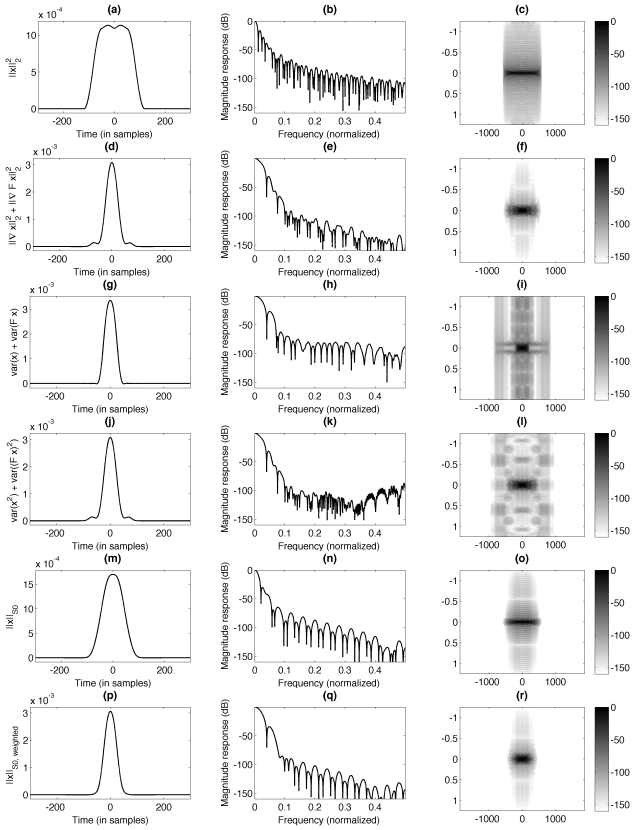

Fig. 9. Results of time-frequency optimization for Exp. 1. The first column shows the time representation, the second the frequency representation and the third the ambiguity function of the window. From top to bottom: canonical dual, gradient, variance, energy variance, S_0 norm, weighted S_0 norm.

	-3 dB-W	ML-W	1/pr-W	SL-A	SL-D
x_{can}	27.5000	1.2292	295.8398	16.3689	106.0177
x_{∇}	8.5000	3.9792	295.6575	31.5146	**124.6016**
x_{var}	**8.1667**	4.0208	**304.5363**	26.6322	70.3673
x_{envar}	8.5000	3.9792	295.6575	31.5040	76.8473
x_{S_0}	16.1667	**2.1042**	293.9675	30.0840	109.6085
$x_{S_0,w}$	8.8333	4.0208	281.5524	**33.9670**	120.2623

TABLE III
WINDOW QUALITY MEASURES FOR THE SOLUTION DUAL WINDOWS. ROWS INDICATE THE DIFFERENT SOLUTIONS WINDOWS, COLUMNS ARE THE VARIOUS CRITERIA (FROM LEFT TO RIGHT): -3 DB WIDTH IN TIME (IN PERCENT OF L_h), MAIN LOBE WIDTH IN FREQUENCY (IN PERCENT OF THE FULL FREQUENCY RANGE) AND THE RECIPROCAL VALUE OF THEIR PRODUCT (PROVIDING A MEASURE OF JOINT TF CONCENTRATION), SIDE LOBE ATTENUATION IN FREQUENCY (IN DB) AND SIDE LOBE DECAY (IN DB, MEASURED AS THE AMPLITUDE DIFFERENCE OF THE MAXIMUM SIDELOBE AND THE LARGEST OF THE 3 FINAL SIDE LOBES BELOW THE NYQUIST FREQUENCY). BEST RESULTS (EXCLUDING THE CANONICAL DUAL FOR THE FIRST 2 MEASURES) ARE INDICATED IN BOLD.

to provide a more diverse set of examples, we exchanged the Tukey window for an Itersine window. Based on the good results in Exp. 1, we selected the time and frequency gradient priors to control the TF spread and optimize

$$\underset{x \in \mathcal{C}_{\text{dual}} \cap \mathcal{C}_{\text{supp}}}{\arg\min} \ \lambda_1 \|\nabla \mathcal{F} x\|_2^2 + \lambda_2 \|\nabla x\|_2^2$$

for varying $\lambda_1, \lambda_2 \in \mathbb{R}^+$, therefore balancing the both concentration measures against one another. Recall that $\|\nabla \mathcal{F} x\|_2^2$

	$\frac{\|\nabla x\|_2}{10^4}$	$\frac{\|\nabla \mathcal{F} x\|_2}{10^4}$	$\frac{\text{var}(\|x\|)}{100}$	$\frac{\text{var}(\|\mathcal{F}x\|)}{100}$	$\frac{\sqrt{\text{var}(\|x\|^2)}}{10^3}$	$\frac{\sqrt{\text{var}(\|\mathcal{F}x\|^2)}}{10^3}$	$\|x\|_{S_0}$	$\|x\|_{S_0,w}$	$\frac{\|x\|_1}{100}$	$\frac{\|\mathcal{F}x\|_1}{10}$	$\frac{\|x\|_2}{10}$
x_{can}	**0.2074**	3.2155	40.0898	0.3523	17.7331	**1.1433**	1.3883	1.4859	**1.3638**	1.8670	**0.5422**
x_{∇}	0.6638	1.4988	8.2516	0.8612	8.2638	3.6602	1.4294	0.7527	1.9182	1.6855	1.1069
x_{var}	0.7941	1.5037	**4.2567**	1.6165	8.2908	4.3791	1.5032	0.7163	2.0872	1.6718	1.2612
x_{envar}	0.6662	**1.4978**	8.2108	0.9996	**8.2580**	3.6734	1.4310	0.7534	1.9213	1.6852	1.1096
x_{S_0}	0.2796	2.1551	18.1214	**0.2434**	11.8833	1.5418	**1.2881**	0.9455	1.4952	1.7094	0.6397
$x_{S_0,w}$	0.6498	1.5361	5.8810	0.8149	8.4695	3.5830	1.4092	**0.6866**	1.9418	**1.6681**	1.0987

TABLE II
TIME AND FREQUENCY CONCENTRATION MEASURES FOR THE SOLUTION DUAL WINDOWS. COLUMNS ARE THE VARIOUS CRITERIA, ROWS INDICATE THE DIFFERENT SOLUTIONS WINDOWS. NOTE THAT THE CRITERIA HAVE BEEN SCALED WITH APPROPRIATE POWERS OF 10 TO IMPROVE READABILITY OF THE TABLE. BEST RESULTS ARE INDICATED IN BOLD.

leads to concentration in time, while $\|\nabla x\|_2^2$ promotes concentration in frequency.

The results, presented in Fig. 10 and Tab. IV, demonstrate the large amount of flexibility when choosing the TF concentration trade-off. It also shows that extreme demands on either time or frequency concentration come at the cost of other properties. In this particular example, time concentration comes at the cost of worse sidelobe attenuation, while strong demands on frequency concentration inhibit quick frequency decay. Despite this, all four solution windows behave as expected and show reasonable to very good overall TF concentration.

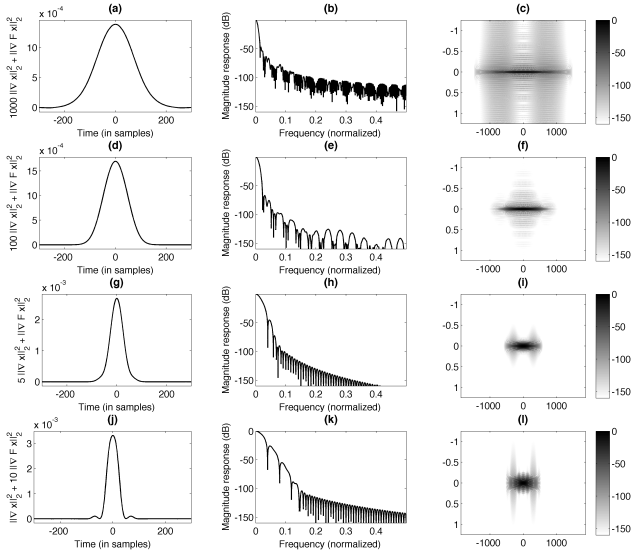

Fig. 10. Results for the TF trade-off experiment optimizing $\lambda_1\|\nabla\mathcal{F}x\|_2^2 + \lambda_2\|\nabla x\|_2^2$. (a)-(c) $\lambda_1 = 1000$, $\lambda_2 = 1$. (d)-(f) $\lambda_1 = 100$, $\lambda_2 = 1$. (g)-(i) $\lambda_1 = 5$, $\lambda_2 = 1$. (j)-(l) $\lambda_1 = 1$, $\lambda_2 = 10$.

Experiment 3 - Smooth dual windows with short support: So far, we have only considered weak support constraints, therefore allowing for a wide variety of dual window choices. Sometimes a stricter constraint is desired, e.g. to reduce delay in real-time application or to minimize the required number of multiplication operations. For fixed redundancy, reducing the time step and the number of frequency channels is computationally cheaper than an increase of the number of frequency channels (amounting to a longer FFT length). Therefore, we consider a non-painless setup, i.e. a system with few frequency channels: $M < L_g$.

	-3 dB-W	ML-W	1/pr-W	SL-A	SL-D
$x_{1/10}$	8.1667	3.9375	621.9631	25.7860	153.8656
$x_{5/1}$	9.8333	4.0208	505.8400	45.0251	161.5928
$x_{100/1}$	18.5000	2.3125	467.4945	66.7578	103.8376
$x_{1000/1}$	28.1667	1.4792	480.0400	46.6063	71.2169

	$\frac{\|\nabla x\|_2}{10^4}$	$\frac{\|\nabla \mathcal{F} x\|_2}{10^4}$
$x_{1/10}$	0.7887	1.5032
$x_{5/1}$	0.5005	1.7009
$x_{100/1}$	0.2365	2.6391
$x_{1000/1}$	0.1545	4.1818

TABLE IV
WINDOW QUALITY MEASURES AND PRIOR VALUES FOR THE SOLUTION WINDOWS OF THE TF TRADE-OFF EXPERIMENT. THE SUBSCRIPT REFERS TO THE RATIO λ_1/λ_2 OF REGULARIZATION PARAMETERS.

The construction of dual Gabor windows with short support has been attempted previously, e.g. by the truncation method in [53], cf. Section III. However, the solutions obtained, are often badly localized in frequency. This is a result of the truncation method yielding to nonsmooth solutions, i.e. solutions with "jumps" or discontinuity-like behaviour in time. By solving the optimization problem Eq. (10) with suitably chosen priors f_i, better results can be obtained, showing reasonable smoothness and therefore frequency concentration.

We start from a Gabor system $\mathcal{G}(g, 30, 60)$ with redundancy 2. The analysis window g is chosen as a Nuttall window of length $L_g = 120$ samples[8].

We desire a dual window h with the same support as g, i.e. $L_h = L_g = 120$. Furthermore, we aim to achieve localization and smoothness by selecting the priors $f_1 = \|\cdot\|_1$,$f_2 = \|\mathcal{F}(\cdot)\|_1$, $f_3 = \|\nabla(\cdot)\|_2^2$ and $f_4 = \|\nabla\mathcal{F}(\cdot)\|_2^2$. Here, f_3, f_4 have been chosen to induce smoothness and localization, while f_1, f_2 have been added to improve the shape of the window, in particular they serve as a counter to the solution's tendency to have multiple peaks. This is unwanted as it leads to windows with ambiguous temporal or frequency position. Heuristically,

[8]The Nuttall window [42] is a compactly supported 4-term window of the form $\chi_{[-0.5,0.5]}\sum_{k=0}^{3} c_k \cos(2k\pi\cdot)$, with $c_0 = 0.355768$, $c_1 = 0.487396$, $c_2 = 0.144232$ and $c_3 = 0.012604$. It has very good side lobe attenuation and decay properties, but is less popular than the widespread Hann and Blackman windows. However, out of those three windows, it best approximates the Gaussian and optimizes all the joint TF concentration measures discussed in Sec. III-A (see webpage).

minimizing the l^1-norm pushes all big coefficients to similar values, therefore achieving the suppression of multiple significant peaks.

The results in Figure 11(c)(d) show the optimal dual window with regards to the regularization parameters $\lambda_1 = \lambda_2 = 0.001$ and $\lambda_3 = \lambda_4 = 1$, chosen experimentally to provide a good result. As reference, we included the least-squares solution provided by the truncation method, see Figure 11(e)(f). At closer examination, we see that the improved sidelobe decay of the optimized dual window comes at the cost of 5dB of side lobe attenuation, compared to the least squares solution, cf. Table V.

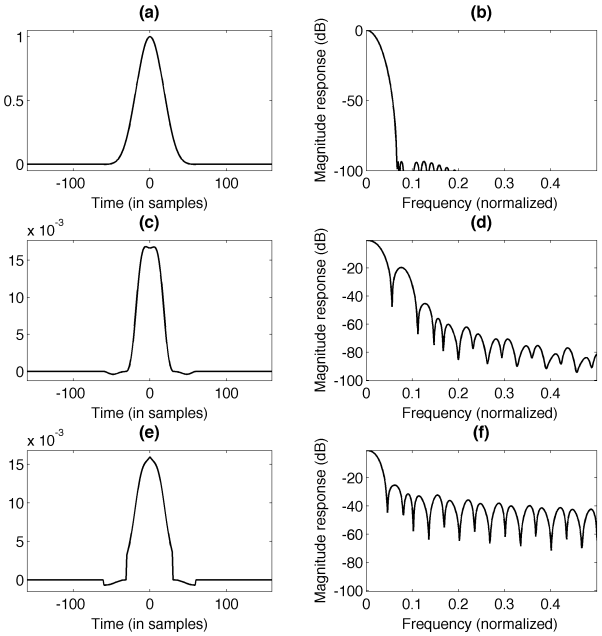

Fig. 11. Experiments. (a)(b) Analysis window in time and frequency. (c)(d) Optimized synthesis window in time and frequency. (e)(f) Truncation method result in time and frequency.

	-3 dB-W	ML-W	1/pr-W	SL-A	SL-D
x_{trunc}	34.1667	**4.6875**	**124.8730**	**24.6729**	20.3697
x_{opt}	**29.1667**	5.7292	119.6883	19.4349	**69.4470**

	$\frac{\|\nabla x\|_2}{100}$	$\frac{\|\nabla \mathcal{F}x\|_2}{100}$	$\|x\|_1$	$\|\mathcal{F}x\|_1$
x_{trunc}	0.6156	2.8254	**0.9092**	0.6774
x_{opt}	**0.5579**	**2.3705**	0.9278	**0.6188**

TABLE V
WINDOW QUALITY MEASURES AND PRIOR VALUES FOR THE SOLUTION WINDOWS OF THE NON PAINLES EXPERIMENT. THE SUBSCRIPT 'OPT' REFERS TO OPTIMIZATION METHOD AND THE SUBSCRIPT 'TRUNC' TO TRUNCTATION METHOD.

In the setup above, the canonical dual window would have very long, quite possibly infinite support. To guarantee compact support on $L_h = L_g$ for the canonical dual, going to the painless case would increase the number of frequency channels to $M \geqslant 120$ and increase the redundancy twofold, the latter being an unwanted side effect. Alternatively, we could decide to keep the parameters $a = 30$, $M = 60$ fixed, but decrease the window size to $L_g \leqslant 60$ for a painless case setup. However, this construction provides a system with a more than 8 times larger frame bound ratio. Consequently, the resulting canonical dual window, shown in Figure 12, shows bad frequency behavior and multiple significant peaks in time. In contrast, the method proposed in this manuscript allows the construction of nicely shaped, compactly supported dual Gabor windows at low redundancies, without the strong restrictions of the painless case.

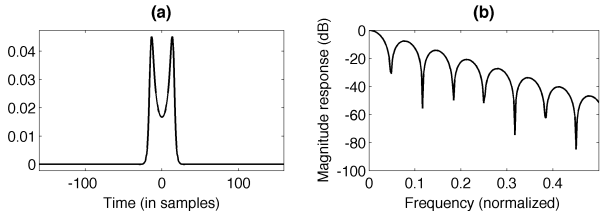

Fig. 12. Half-overlap painless case construction ($\mathcal{G}(g, 30, 60)$, $L_g = 60$): Canonical dual window in time (a) and in frequency (b).

Excursion - Improvement of classical tight frame constructions:

Sometime significant simplifications of applications or algorithms are achieved, whenever tight frames are used, e.g. the ℓ^1 regularized least-squares using the SALSA algorithm [3]. Instead of computing the dual window to a previously selected analysis window, we now attempt the computation of a *Gabor Parseval frame*[9] with good properties, given the parameters a, M. A system $\mathcal{G}(h, a, M)$ is a Parseval frame, if it is a dual frame to itself. We consider only Parseval frames, since every tight frame is Parseval up to a scaling factor. The Gabor Parseval windows h for parameters a, M are characterized by the nonlinear equation system

$$\frac{M}{a}\left\langle h, h[\cdot - nM]e^{2\pi im\cdot/a}\right\rangle = \delta[n]\delta[m],$$

obtained by setting $g = h$ in the WR equations (8). The solution set associated to this equation system is not convex. Indeed, little is known about the set beyond it being a pathwise connected [36] subset of $\{h \in \ell_2(\mathbb{Z}) \ : \ \|h\|_2^2 = a/M\}$. Even worse, since we only consider real-valued solution windows, the connectedness property might be violated. Although no convergence guarantees can be given, we will provide a heuristic optimization scheme that provided good experimental results.

In order to implement our proposed scheme, we need a method to compute the projection onto the set of Parseval windows:

$$P_{\mathcal{C}_{\text{Pars}}}(y) = \underset{x \in \mathcal{C}_{\text{Pars}}}{\arg\min} \|x - y\|_2.$$

It can be shown [32] that this projection can be computed via the formula

$$P_{\mathcal{C}_{\text{Pars}}}(y) = \mathbf{S}_{y,a,M}^{-1/2} y, \tag{13}$$

where $\mathbf{S}_{y,a,M}$ is the frame operator with respect to $\mathcal{G}(y, a, M)$, cf. [32]. The result of $\mathbf{S}_{y,a,M}^{-1/2} y$ is called the *canonical tight*

[9] A Parseval frame is a tight frame with frame bound 1.

window and efficient algorithms for its computation are freely available, e.g. in the LTFAT toolbox [51], see also [33]. The canonical tight window always forms a Parseval frame.

We attempt to solve the tight problem with PPXA, simply replacing the projection on the dual set by projection onto the set of Parseval windows. At convergence, a final projection onto the tight set ensures the tightness property of the result. If a support constraint is desired, the final projection is based on a POCS-based algorithm. however, if there is no convergence guarantee of this final step, even if $\mathcal{C}_{\text{Pars}}$ and $\mathcal{C}_{\text{supp}}$ are not disjoint. We have no theoretical guarantee to find a good solution to the problem with this method, since both the PPXA and POCS steps lack a convergence guarantee. Nevertheless, our approach is not blindly random. PPXA, is a generalization of the Douglas-Rachford algorithm [19]. The latter algorithm, when applied to non convex, lower, semi-continuous functions has been proved to converge to stationary point. In fact it is one consequence of a more general minimization scheme presented by Attouch [4]. Unfortunately, the indicator function of the set of real-valued Parseval windows is most likely not semi-continuous and therefore not subject to Attouch's result.

Since the problem is not convex, a good starting value and a good timestep are crucial. We have obtained good results and dependable convergence when choosing a starting window that is not too far from what we aim for, i.e. it already has a good frame bound ratio B/A for the Gabor parameters a, M and shows the properties we wish to promote in the tight window, e.g. TF concentration. Note that, especially for frames with small redundancy, it has been observed that a tradeoff between localization and smoothness in TF exists between the analysis and dual windows. Therefore, low redundancy Parseval frame windows provide, in comparison, suboptimal TF concentration.

As starting setup, we choose a Gabor system $\mathcal{G}(g, 30, 60)$ with an Itersine window of length $L_g = 60$. For this half-overlap, redundancy 2 situation, the Itersine window forms a tight, painless frame with better joint TF concentration than other widely used constructions for redundancy 2 tight frames, such as the cosine window $\chi_{[-0.5,0.5]}\cos(\pi\cdot)$ or rectangular window $\chi_{[-0.5,0.5]}$. We now attempt the construction of a Gabor Parseval frame with redundancy 2, using a window function that further improves the TF concentration of the Itersine window.

To gain some design freedom, we allow the tight window g_t to have support length $L_{g_t} \leqslant 360$. As in the earlier experiments, gradient priors are used to promote a window that is smooth and well-localized in both domains, leading (formally) to the optimization problem

$$\underset{x\in\mathcal{C}_{\text{Pars}}\cap\mathcal{C}_{\text{supp}}}{\arg\min}\ \lambda_1\|\nabla\mathcal{F}x\|_2^2 + \lambda_2\|\nabla x\|_2^2.$$

For easier comparison, we tuned the result to have roughly the same visual concentration in time. The result shown was obtained for the regularization parameters $\lambda_1 = 1,\ \lambda_2 = 5$ and shows improved decay and side lobe attenuation, when compared to the Itersine, see Fig. 13 and Tab. IV.

Although the heuristic tight frame optimization has provided promising results, there is no guarantee for the results' optimality. Whenever the tight frame property is not essential, the construction of a pair of dual frames with good TF concentration might be preferable. For the same parameters as before, we choose a Nuttall window of length $L_g = 120$ to construct a frame. This window is slightly broader in time than the Itersine window used before, but provides very good decay and concentration in frequency, see Figure 14. For the dual window, we consider $L_h \leqslant 360$ as in the tight case and the optimization problem

$$\underset{x\in\mathcal{C}_{\text{dual}}\cap\mathcal{C}_{\text{supp}}}{\arg\min}\ \lambda_1\|\nabla\mathcal{F}x\|_2^2 + \lambda_2\|\nabla x\|_2^2.$$

Again, the regularization parameters have been tuned to provide similar concentration in time. The dual window shown in Fig. 14 was obtained for the regularization parameters $\lambda_1 = 0.1,\ \lambda_2 = 1$. Both the Nuttall window and its optimized dual show improved joint TF concentration over the tight Itersine window, see also Tab. VII. In terms of joint TF localization, the values presented in Tab. IV and Tab. VII suggest that all 3 prototypes constructed in this excursion show a considerable improvement upon the Itersine window and consequently over other widely used redundancy 2 tight Gabor frame constructions.

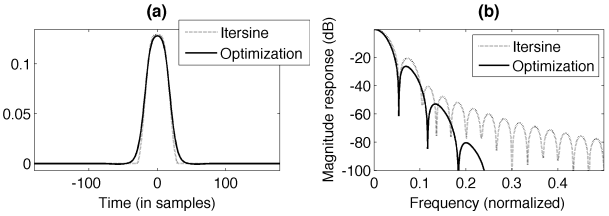

Fig. 13. $\mathcal{G}(g, 30, 60)$, $L_g = 60$, compactly supported tight windows: $L_g = 360$: Itersine (a)(b)(c). Result of optimization (d)(e)(f).

	-3 dB-W	ML-W	1/pr-W	SL-A	SL-D
x_{iter}	10.2778	5.5449	175.4726	20.5885	78.1983
x_{opt}	10.2778	**5.4167**	**179.6258**	**26.1916**	**126.9964**

	$\frac{\|\nabla x\|_2}{100}$	$\frac{\|\nabla\mathcal{F}x\|_2}{100}$
x_{iter}	4.1096	**5.5811**
x_{opt}	**3.5207**	6.0137

TABLE VI
WINDOW QUALITY MEASURES AND GRADIENT CRITERIA FOR THE TIGHT WINDOW EXPERIMENT. THE SUBSCRIPT INDICATES THE WINDOW: x_{ITER}: ITERSINE WINDOW, x_{OPT}: OPTIMIZED TIGHT WINDOW. BEST VALUES INDICATED IN BOLD.

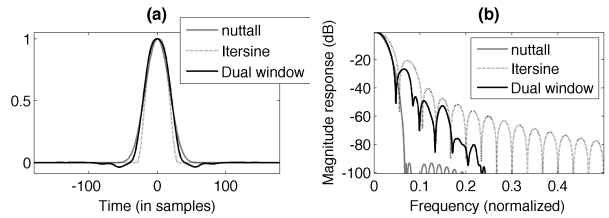

Fig. 14. Construction of a pair of dual FIR windows both improving Itersine TF concentration ($\mathcal{G}(g, 30, 60)$, Itersine $L_g = 60$ (a)(b)(c), Nuttall $L_{g_0} = 120$ (d)(e)(f), Dual window $L_h = 120$ (g)(h)(i)): Left windows in time. Center windows in frequency. Right: ambiguity fonction

	-3 dB-W	ML-W	1/pr-W	SL-A	SL-D
x_{iter}	$\mathbf{10.2778}$	5.5093	$\mathbf{176.6069}$	20.5903	78.1948
x_{nutt}	11.3889	6.7130	130.7990	$\mathbf{93.3292}$	55.7800
x_{opt}	11.9444	$\mathbf{4.7685}$	175.5701	26.0021	$\mathbf{91.1066}$

	$\frac{\|\nabla x\|_2}{100}$	$\frac{\|\nabla \mathcal{F} x\|_2}{100}$
x_{iter}	4.3278	$\mathbf{8.4892}$
x_{nutt}	3.1292	10.5630
x_{opt}	$\mathbf{3.0412}$	9.1353

TABLE VII
WINDOW QUALITY MEASURES AND GRADIENT CRITERIA FOR THE TIGHT WINDOW EXPERIMENT. THE SUBSCRIPT INDICATES THE WINDOW: x_{ITER}: ITERSINE WINDOW, x_{NUTT}: NUTTALL WINDOW, x_{DUAL}: OPTIMIZED DUAL WINDOW. BEST VALUES INDICATED IN BOLD. MINOR DIFFERENCES TO TAB. 1 ARE DUE TO DIFFERENT ASSUMED LENGTH L. THEY AMOUNT TO EITHER SAMPLING ISSUES (ML-W) OR A SCALING FACTOR ($\|\nabla \mathcal{F} x\|_2$).

V. CONCLUSION

In this contribution, we have proposed a convex optimization framework for the computation of optimized Gabor dual windows. The presented method is based on the observation that the set of dual windows for a fixed Gabor filterbank can be described as the solution set to the linear Wexler-Raz equations. Furthermore, we exploit the facts that support constraints can be expressed as linear equations and that compactly supported Gabor windows are dual independent of the underlying signal length.

The resulting scheme enables the computation of alternative dual windows, with the possibility to optimize a wide variety of criteria, freely chosen by the user. Although the complexity varies with the selected priors, results are usually obtained efficiently using the provided open-source implementation, supplied on the associated webpage http://unlocbox.sourceforge.net/rr/gdwuco.

We provided several demonstrations of the method's capability in the context of joint time-frequency concentration optimization. In particular, we constructed dual windows that considerably improve time-frequency concentration over the widely used canonical dual, windows that provide alterative ratios between time and frequency concentration and windows that combine short support, smoothness and frequency concentration. Finally, we showed that we can, heuristically, apply the proposed framework to compute well-concentrated tight windows, improving previously known explicit tight frame consructions.

The results show that our method can be applied in various situations to construct dual frames with properties more relevant for application than minimal ℓ^2-norm.

Future work will concern the extension of the presented scheme to more general systems, e.g. Gabor systems with complex-valued window on nonseparable sampling sets [56] and nonstationary Gabor frames [6].

Acknowledgement

This work was supported by the Austrian Science Fund (FWF) START-project FLAME ("Frames and Linear Operators for Acoustical Modeling and Parameter Estimation"; Y 551-N13).

REFERENCES

[1] A. Adler, V. Emiya, M. Jafari, M. Elad, R. Gribonval, and M. Plumbley. A constrained matching pursuit approach to audio declipping. In *IEEE International Conference on Acoustics, Speech and Signal Processing (ICASSP)*, pages 329–332. IEEE, 2011.

[2] A. Adler, V. Emiya, M. Jafari, M. Elad, R. Gribonval, and M. Plumbley. Audio inpainting. *IEEE Transactions on Audio, Speech, and Language Processing*, 20(3):922–932, 2012.

[3] M. Afonso, J. Bioucas-Dias, and M. A. T. Figueiredo. Fast image recovery using variable splitting and constrained optimization. *Image Processing, IEEE Transactions on*, 19(9):2345–2356, Sept 2010.

[4] H. Attouch, J. Bolte, P. Redont, and A. Soubeyran. Proximal alternating minimization and projection methods for nonconvex problems: An approach based on the kurdyka-lojasiewicz inequality. *Mathematics of Operations Research*, 35(2):438–457, 2010.

[5] P. Balazs. Basic definition and properties of Bessel multipliers. *Journal of Mathematical Analysis and Applications*, 325(1):571–585, January 2007.

[6] P. Balazs, M. Dörfler, N. Holighaus, F. Jaillet, and G. Velasco. Theory, implementation and applications of nonstationary Gabor frames. *Journal of Computational and Applied Mathematics*, 236(6):1481–1496, 2011.

[7] P. Balazs, M. Dörfler, M. Kowalski, and B. Torrésani. Adapted and adaptive linear time-frequency representations: a synthesis point of view. *IEEE Signal Processing Magazine (special issue: Time-Frequency Analysis and Applications)*, to appear:–, 2013.

[8] P. Balazs, H. G. Feichtinger, M. Hampejs, and G. Kracher. Double preconditioning for Gabor frames. *IEEE T. Signal. Proces.*, 54(12):4597–4610, December 2006.

[9] H. Bölcskei. A necessary and sufficient condition for dual Weyl-Heisenberg frames to be compactly supported. *J. Fourier Anal. Appl.*, 5(5):409–419, 1999.

[10] H. Bölcskei and F. Hlawatsch. Oversampled cosine modulated filter banks with perfect reconstruction. *IEEE Trans. Circuits and Systems II*, 45(8):1057–1071, Aug. 1998.

[11] S. Boyd, N. Parikh, E. Chu, B. Peleato, and J. Eckstein. Distributed optimization and statistical learning via the alternating direction method of multipliers. *Foundations and Trends® in Machine Learning*, 3(1):1–122, 2011.

[12] S. S. Chen, D. L. Donoho, and M. A. Saunders. Atomic Decomposition by Basis Pursuit. *SIAM Journal on Scientific Computing*, 20(1):33–61, Jan. 1998.

[13] O. Christensen. Pairs of dual Gabor frame generators with compact support and desired frequency localization. *Appl. Comput. Harmon. Anal.*, 20(3):403–410, 2006.

[14] O. Christensen. *Frames and Bases. An Introductory Course.* Applied and Numerical Harmonic Analysis. Basel Birkhäuser, 2008.

[15] O. Christensen and S. Goh. Pairs of dual periodic frames. *Appl. Comput. Harmon. Anal.*, 33(3):315 – 329, November 2012.

[16] O. Christensen, H. Kim, and R. Y. Kim. Gabor windows supported on $[-1, 1]$ and compactly supported dual windows. *Appl. Comput. Harmon. Anal.*, 28(1):89 – 103, January 2010.

[17] O. Christensen, H. Kim, and R. Y. Kim. Gabor windows supported on [-1, 1] and dual windows with small support. *Adv. Comput. Math.*, 36(4):525–545, 2012.

[18] O. Christensen and R. Kim. On dual Gabor frame pairs generated by polynomials. *J. Fourier Anal. Appl.*, 16(1):1–16, 2010.

[19] P. Combettes and J. Pesquet. A Douglas–Rachford splitting approach to nonsmooth convex variational signal recovery. *IEEE Journal of Selected Topics in Signal Processing*, 1(4):564–574, 2007.

[20] P. Combettes and J. Pesquet. Proximal splitting methods in signal processing. *Fixed-Point Algorithms for Inverse Problems in Science and Engineering*, pages 185–212, 2011.

[21] P. Combettes and V. Wajs. Signal recovery by proximal forward-backward splitting. *Multiscale Modeling & Simulation*, 4(4):1168–1200, 2005.

[22] P. L. Combettes. The foundations of set theoretic estimation. *Proceedings of the IEEE*, 81(2):182–208, 1993.

[23] I. Daubechies, H. J. Landau, and Z. Landau. Gabor Time-Frequency Lattices and the Wexler-Raz Identity. *Journal of Fourier Analysis and Applications*, 1(4):437–478, Nov. 1994.

[24] H. G. Feichtinger. On a new Segal algebra. *Monatsh. Math.*, 92:269–289, 1981.

[25] H. G. Feichtinger and K. Nowak. *A first survey of Gabor multipliers*, chapter 5, pages 99–128. 2003.

[26] H. G. Feichtinger and T. Strohmer, editors. *Gabor Analysis and Algorithms*. Birkhäuser, Boston, 1998.

[27] K. Gröchenig. *Foundations of Time-Frequency Analysis*. Appl. Numer. Harmon. Anal. Birkhäuser Boston, Boston, MA, 2001.
[28] K. Gröchenig and J. Stöckler. Gabor frames and totally positive functions. *Duke Math. J.*, 162(6):1003–1031, 2013.
[29] W. W. Hager and H. Zhang. A survey of nonlinear conjugate gradient methods. *Pacific journal of Optimization*, 2006.
[30] F. Harris. On the use of windows for harmonic analysis with the discrete fourier transform. *Proceedings of the IEEE*, 66(1):51–83, Jan 1978.
[31] A. Janssen and P. L. Søndergaard. Iterative algorithms to approximate canonical Gabor windows: Computational aspects. *J. Fourier Anal. Appl.*, 13(2):211–241, 2007.
[32] A. Janssen and T. Strohmer. Characterization and computation of canonical tight windows for gabor frames. *Journal of Fourier Analysis and Applications*, 8(1):1–28, 2002.
[33] A. J. E. M. Janssen and T. Strohmer. Characterization and computation of canonical tight windows for Gabor frames. *J. Fourier Anal. Appl.*, 8(1):1–28, January 2002.
[34] M. Kowalski, K. Siedenburg, and M. Dörfler. Social sparsity! neighborhood systems enrich structured shrinkage operators. *Signal Processing, IEEE Transactions on*, 61(10):2498–2511, 2013.
[35] F. Krahmer, G. Kutyniok, and J. Lemvig. Sparsity and spectral properties of dual frames. *Linear Algebra and its Applications*, 439(4):982 – 998, 2013. 17th Conference of the International Linear Algebra Society, Braunschweig, Germany, August 2011.
[36] D. Labate and E. Wilson. Connectivity in the set of Gabor frames. *Appl. Comput. Harmon. Anal.*, 18(1):123–136, 2005.
[37] R. S. Laugesen. Gabor dual spline windows. *Appl. Comput. Harmon. Anal.*, 27(2):180 – 194, September 2009.
[38] S. Li, Y. Liu, and T. Mi. Sparse Dual Frames and Dual Gabor Functions of Minimal Time and Frequency Supports. *Journal of Fourier Analysis and Applications*, pages 1–29, 2012.
[39] H. S. Malvar. *Signal Processing with Lapped Transforms*. Artech House Publishers, 1992.
[40] B. Martinet. Détermination approchée d'un point fixe d'une application pseudo-contractante. cas de l'application prox. *CR Acad. Sci. Paris Ser. AB*, 274:A163–A165, 1972.
[41] G. Matz and F. Hlawatsch. *Linear Time-Frequency Filters: On-line Algorithms and Applications*, chapter 6 in 'Application in Time-Frequency Signal Processing', pages 205–271. eds. A. Papandreou-Suppappola, Boca Raton (FL): CRC Press, 2002.
[42] A. Nuttall. Some windows with very good sidelobe behavior. *Acoustics, Speech and Signal Processing, IEEE Transactions on*, 29(1):84–91, 1981.
[43] N. Perraudin, N. Holighaus, P. Soendergaard, and P. Balazs. Gabor dual windows using convex optimization. In *Proceeedings of the 10th International Conference on Sampling theory and Applications (SAMPTA 2013)*, 2013.
[44] N. Perraudin, D. Shuman, G. Puy, and P. Vandergheynst. UNLocBoX A matlab convex optimization toolbox using proximal splitting methods. *ArXiv e-prints*, Feb. 2014.
[45] H. Raguet, J. Fadili, and G. Peyre. Generalized Forward-Backward Splitting. *arXiv.org*, Aug. 2011.
[46] B. Ricaud and B. Torrésani. A survey of uncertainty principles and some signal processing applications. *Advances in Computational Mathematics*, pages 1–22, 2013.
[47] R. Rockafellar. Monotone operators and the proximal point algorithm. *SIAM Journal on Control and Optimization*, 14(5):877–898, 1976.
[48] S. Samadi, M. O. Ahmad, and M. N. S. Swamy. Characterization of nonuniform perfect-reconstruction filterbanks using unit-step signal. *IEEE Transactions on Signal Processing*, 52(9):2490–2499, 2004.
[49] S. Setzer, G. Steidl, and T. Teuber. Deblurring poissonian images by split bregman techniques. *Journal of Visual Communication and Image Representation*, 21(3):193 – 199, 2010.
[50] P. L. Søndergaard. Gabor frames by Sampling and Periodization. *Adv. Comput. Math.*, 27(4):355 –373, 2007.
[51] P. L. Søndergaard, B. Torrésani, and P. Balazs. The Linear Time Frequency Analysis Toolbox. *International Journal of Wavelets, Multiresolution Analysis and Information Processing*, 10(4), 2012.
[52] D. T. Stoeva and P. Balazs. Invertibility of multipliers. *Applied and Computational Harmonic Analysis*, 33(2):292–299, 2012.
[53] T. Strohmer. Numerical algorithms for discrete Gabor expansions. In Feichtinger and Strohmer [26], chapter 8, pages 267–294.
[54] M. Vetterli. Filter banks allowing perfect reconstruction. *Signal Process.*, 10:219–244, 1986.
[55] J. Wexler and S. Raz. Discrete Gabor expansions. *Signal Processing*, 21(3):207–220, Nov. 1990.
[56] C. Wiesmeyr, N. Holighaus, and P. Sondergaard. Efficient algorithms for discrete Gabor transforms on a nonseparable lattice. *IEEE Trans. Signal Process.*, 61(20):5131 – 5142, 2013.

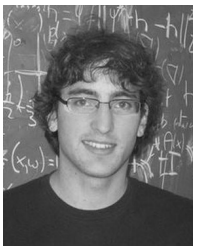

N. Perraudin studied electrical engineering at EPFL ("Ecole polytechnique fédéral de Lausanne") where he specialized himself in signal processing. After his degree he spent six months as research assistant at the Acoustic Research Institute at the Austrian Academy of Science. Then, in 2013, he started a PHD at LTS2 (laboratoire de traitement du signal) at EPFL. His current research focuses on three different domains: spectral graph theory, convex optimization and Gabor analysis.

He is the founder and the maintainer of open-source project called the UNLocBoX (A matlab convex optimization toolbox): http://unlocbox.sourceforge.net/.

N. Holighaus studied mathematics and theoretical computer sciences at Justus–Liebig–University, Gießen, Germany. In 2013 he received his Ph.D. degree in mathematics at the University of Vienna, where he worked from 2010 to 2012 as research assistant at the Numerical Harmonic Analysis Group (NuHAG), Faculty of Mathematics. Since August 2012 he works as a research assistant at the Acoustic Research Institute at the Austrian Academy of Sciences.

His research interests include applied frame theory and time-frequency analysis, adaptive time-frequency techniques and signal processing.

P. Søndergaard studied applied time-frequency analysis at the Technical University of Denmark. He defended his Ph.D. thesis on "Finite Discrete Gabor Analysis" in 2007. From 2007 - 2012 he worked at the Centre for Applied Hearing Research in Denmark, working with auditory modeling and accurate signal modifications. From 2012 to 2013 he lead the 'Mathematics and Signal Processing in Acoustics' group at the Acoustic Research Institute (ARI) at the Austrian Academy of Sciences. He is currently employed at Oticon R&D since August 2013.

He is the creator of the two open-source software projects, The Large Time Frequency Toolbox, LTFAT: http://ltfat.sourceforge.net/ and the Auditory Modeling Toolbox, AMToolbox: http://amtoolbox.sourceforge.net/, which are maintained by ARI.

P. Balazs (M'01 S'12) received the Ph.D. degree (2005) and the habilitation (2011) degree in mathematics at the University of Vienna, in cooperation with the Numerical Harmonic Analysis Group. He has been a member of the Acoustics Research Institute (ARI) of the Austrian Academy of Sciences since 1999. He also worked at the Laboratoire d'Analyse Topologie et Probabilités and the Laboratoire de Mécanique et d'Acoustique, in Marseille, France, from 2003 to 2006 as well as the Unité de physique théorique et de physique mathématique (FYMA) from the Université Catholique de Louvain à Louvain-La-Neuve. He is the founder of the working group 'Mathematics and Acoustical Signal Processing' at ARI. He has been the director of ARI since 2012. He is interested in time-frequency analysis, Gabor analysis, numerical analysis, frame theory, signal processing, acoustics, and psychoacoustics.